Communication

The Effect of "Wave Breakers" on the Magnetohydrodynamic Instability in Aluminum Reduction Cells

ALEX PEDCENKO, SERGEI MOLOKOV, and BENOIT BARDET

We report the results of the experiments on the suppression of the MHD instability in a model of the aluminum reduction cells (Pedchenko *et al.* in EPL 88:24001, 2009). The idea behind the study is to introduce obstacles in the liquid metal to suppress the propagation of the rolling-pad instability wave. As a result, in some configurations with obstacles, we detect lowering of the wave amplitude, reduction of its propagation speed, and rise of the main parameters' thresholds, responsible for the instability onset.

DOI: 10.1007/s11663-016-0840-5

The effective control of magnetohydrodynamic (MHD) instabilities in aluminum reduction cells is the problem of great importance. The process of primary aluminum production (aluminum smelting) is based on the electrolytic reduction of the metallic aluminum from its high melting point oxide: alumina [2345 K (2072 °C)]. In this technology, known as Hall-Héroult process, the alumina is dissolved in molten cryolite,* which lowers its melting point and improves its electric conductivity. This solution is contained at 1233 K (960°C) in large (*e.g.*, 13 × 4 × 0.3 m) rectangular cells—electrolytic pots, with graphite top and bottom lining, serving as the anode and cathode electrodes, respectively. High electric current of several hundreds kA is then passed through the cell, and, as a result of the electrochemical reaction, the liquid aluminum "pad" is formed under the cryolite, at the bottom of the cell. The process is relatively expensive due to the amount of electricity required for the reduction of each kilogram of aluminum (11 to 14 kWh). The main loss of energy is due to low electric conductivity of cryolite, so reducing its thickness by every millimeter can result in substantial savings worldwide.

Unfortunately, when the cryolite thickness** is reduced below a certain threshold, such a binary system of two immiscible fluids with the vast difference in their electrical conductivities and very small difference in densities become unstable owing to the electromagnetic body force. This force appears due to the interaction of the horizontal component of the electric current and vertical component of the background magnetic field, produced by the bus bars supplying electricity to the cell. This interfacial instability, being magnetohydrodynamic in nature, is known to produce sloshing or "rolling-pad" waves[4] at the interface between the cryolite and aluminum, propagating along the perimeter of the cell in a rotating fashion. Such disturbances of the interface can reduce effectiveness of the smelting process and disrupt the normal operation of the cell or even the whole pot-line. Thus, the control and suppression of unstable surface waves is one of the important problems in aluminum smelting.

Since pioneering work by Sele,[4] who identified the basic mechanism for the interface motion, many theoretical studies were devoted to the understanding of the impact of different technological factors on the fluid motion in the aluminum layer. Experimental investigation of the phenomenon, however, is quite complicated due to the lack of safe and accessible experimental modeling materials with the required physical properties. One of the possible solutions proposed in Reference 1 is to replace in the model the poorly conducting cryolite with an array of 30 × 30, ⌀2-mm-thin, vertical stainless steel electrodes, which when immersed in the liquid metal, supply the electric current to its free surface and do not obstruct its vertical motion. Because the effective electric resistance of such an array of thin conductors is about 100 times higher than that of liquid metal, the tilt of the interface will result in the redistribution of the electric current between all parallel electrodes. This creates a horizontal component of the current $j_\perp$ in the better conducting liquid metal, as the current needs to spread there before entering less conductive bottom of the cell. Externally imposed vertical magnetic field $\vec{B}$ of a sufficient strength (up to 100 mT) triggers a horizontal motion of the liquid metal due to the appearance of the electromagnetic Lorentz

*sodium aluminum fluoride salt

**known also as the anode to cathode distance, ACD

ALEX PEDCENKO, Senior Lecturer in Applied Physics, and SERGEI MOLOKOV, Professor in Applied Mathematics, are with Coventry University, Priory Street, Coventry, UK. Contact e-mails: a.pedcenko@coventry.ac.uk, aa3025@coventry.ac.uk BENOIT BARDET, Modeling Research Engineer, is with Rio Tinto LRF, rue Henri Sainte Claire Deville, CS 40114, 73302 St-Jean-de-Maurienne cedex, France.

Manuscript submitted June 16, 2016.
Article published online November 4, 2016.

force $\vec{J} \wedge \vec{B}$, eventually resulting in the rolling surface wave with a growing amplitude. Such a physical model does not pretend to replicate the entirety of electrodynamic processes occurring in the real cell, but it mimics the basic principle of the Sele-type MHD instability and thus is dynamically similar to the instability in real cells. The advantages of this experimental model have been discussed in Reference 1. The present report is an extension of the previous experimental study published in Reference 1 and modeling work presented in Reference 2.

One of the possible ways to suppress the sloshing motion of a fluid is to introduce obstacles (*i.e.*, "wave breakers"). For example, partitioning walls or baffles are used in tankers to suppress a surge or sloshing of liquids during transportation.

Song *et al.*[5] report some slowing down of the liquid metal using "cathode with protrusions" in both numerical and industrial trials. Dupuis and Bojarevics[6,7,8] report that the overall damping effect is not that significant, but all agree that such protrusions can increase the horizontal current in the liquid metal, which is responsible for the instability onset. It seems that the balance between these two effects will determine the success or otherwise of such a cathode construction. In our study, we use non-conductive "protrusions," which have no influence on the current distribution in the liquid metal, and their role is purely hydrodynamic.

The experimental cell (Figure 2) used in this work has the same construction as in Reference 1: 30×30 cm square box filled with 2 to 5 cm thick layer of room-temperature liquid metal alloy In-Ga-Sn. To prevent the oxidation of liquid metal and overheating of thin anode electrodes, the gap between the free surface of the liquid metal and the top anode plate was filled with weak 3 pct HCl water solution. As the obstacles (further referred to as WB), the identical plexiglass bars of the 10×15 mm cross-section, placed across the width of the cell and attached to its bottom, were used. In different tests, their number (from 1 to 7) and the arrangement were changed. Figure 1(a) shows schematic view of the experimental cell with only one WB in the middle, while Figure 1(b) shows 3D view of the cell with 5 WB uniformly spread along its bottom. The external uniform vertical magnetic field (10 to 80 mT) generated by two induction coils was applied throughout the cell.

The height of WB was kept the same 1.5 cm in all the trials and was chosen to be less than the minimum height of the liquid metal layer (2 cm) in order not to partition the cell into separate compartments, but to allow the motion of liquid metal across the whole cell.

The measurements of free surface oscillations in the unstable regime of the cell were taken for different WB configurations and melt heights. Recordings were performed using video camera (Figure 2), which was filming the middle area of the front wall of the cell at 30 fps. This allowed us to detect the instantaneous height of the liquid metal at that particular location during the passage of the wave. Later, the video data were post-processed, and the time-history of the surface oscillations extracted with the accuracy of about ± 0.1 mm.

Before introducing any obstacles in the melt, the test case without them was recorded for every height of the liquid metal layer (h_0 = 20, 35, and 50 mm) at different values of the anode current I and vertical magnetic field B. This case served as a reference data for later tests with different WB arrangements (Figure 3). Normally, in a single test run for one height of the melt, different WB configurations were tested. To keep the melt level constant, the small amount of In-Ga-Sn alloy was taken out or added into the cell in order to compensate for the volume occupied by WB.

The general procedure was the following: the desired WB arrangement was installed in the cell and the required height of the melt was set. The top anode plate with 900 stainless steel electrodes (see Figure 2) was lowered for the tips of the electrodes to immerse into the liquid metal for 1 ± 0.25 mm below the free surface. Then relatively high values of the anode current I and the magnetic field B were set to trigger the onset of the wave.

After that, both I and B were lowered to the desired values. Then the magnetic field was kept constant and the current I was lowered in small steps. At each step of the current magnitude, a video recording of the surface oscillations was taken. Then the procedure was repeated

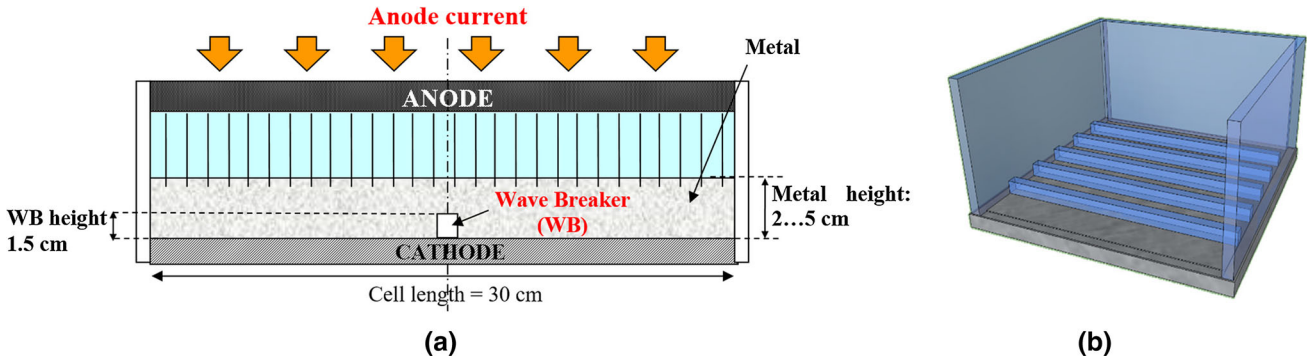

Fig. 1—(*a*) Side view of the experiment with 1 WB installed in the middle of the cell; (*b*) 3D view of the cell (one side wall removed) with 5 WB equally spaced along its width.

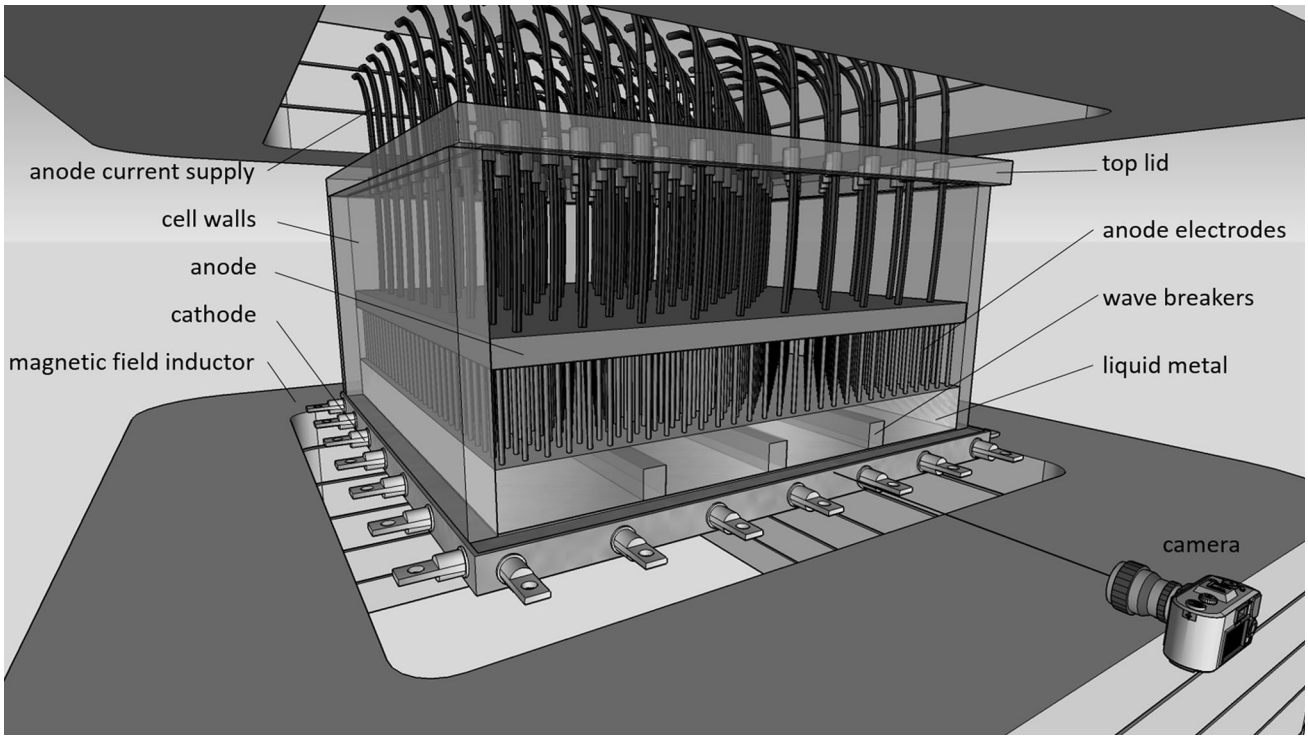

Fig. 2—3D view of the test cell inside the inductor coils (color online).

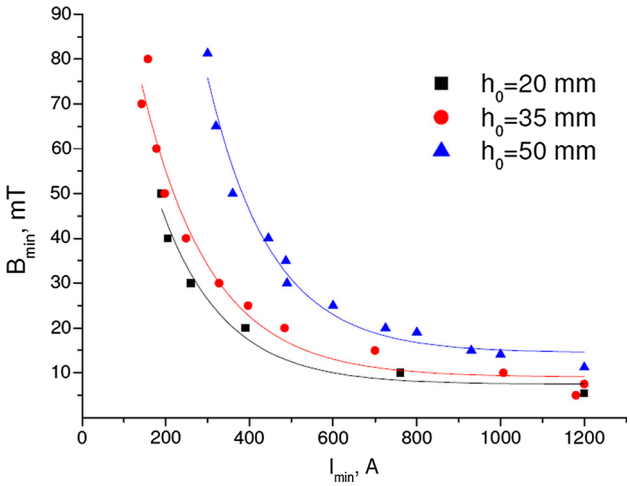

Fig. 3—Lower threshold curves of $B(I)$ for three melt levels h_0 = 20, 35, and 50 mm without "wave breakers".

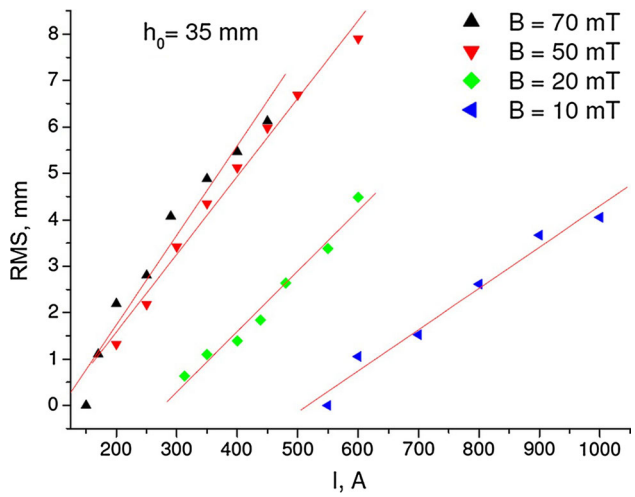

Fig. 4—RMS value of the surface oscillations *vs.* anode current I, A for different values of magnetic field B, and single melt height h_0 = 35 mm without "wave breakers".

for a different magnetic field value B, and so on. For each B, a certain minimum value of the anode current $I_{\min}$ was found, at which the cell became stable. This pair of $B_{\min}$ and $I_{\min}$ values was recorded as the "*lower thresholds*." The set of such $B_{\min}$ and $I_{\min}$ combinations was found for each WB arrangement and represented the stability curve, below which the cell is stable.

Figure 3 shows the reference case of lower threshold values B and I for when no WBs were installed in the cell. The magnetic field was varied between 5 and 80 mT, and the anode current was varied between 100 and 1200 A. The uncertainty of each experimental point on this graph, *i.e.,* of finding the lowest $I_{\min}$ value while keeping B constant, is several amperes.

One can see that the curves follow some sort of inverse function $\sim I^{-1}$, and the higher melt level h_0 generally leads to a more stable cell. The amplitude of the wave is proportional to the product of B and I.

Figure 4 shows the standard deviation of the free surface oscillations, obtained from the video recordings, as a function of the anode current I and the magnetic field B for one height of the melt (35 mm). The

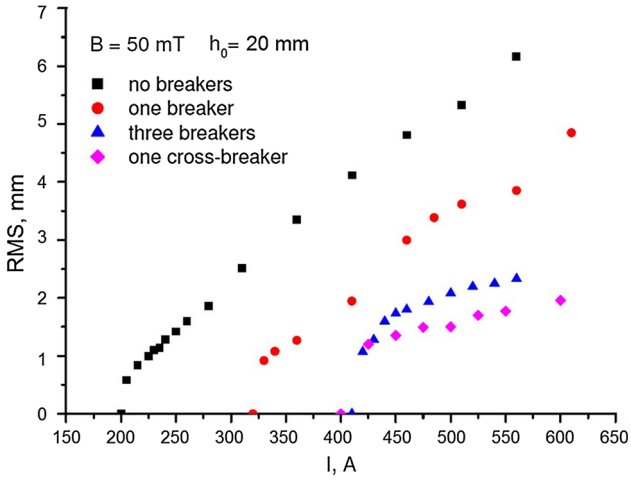

Fig. 5—RMS value of the surface oscillations vs. anode current I, A for magnetic field, $B = 50$ mT, and melt height $h_0 = 20$ mm with different WB arrangement.

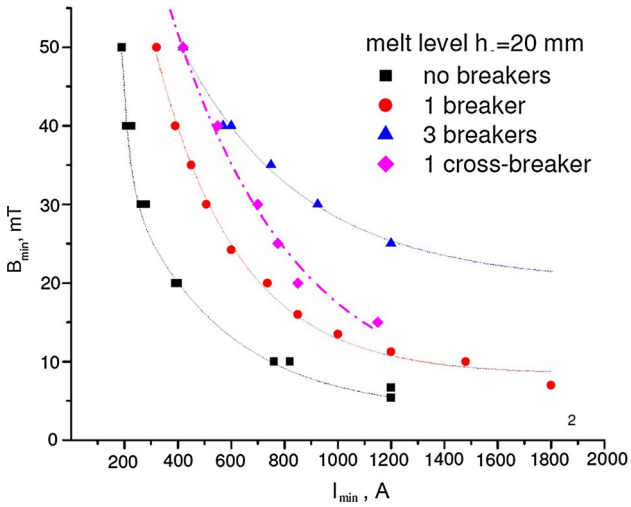

Fig. 6—Stability thresholds for melt level $h_0 = 20$ mm and different WB arrangements.

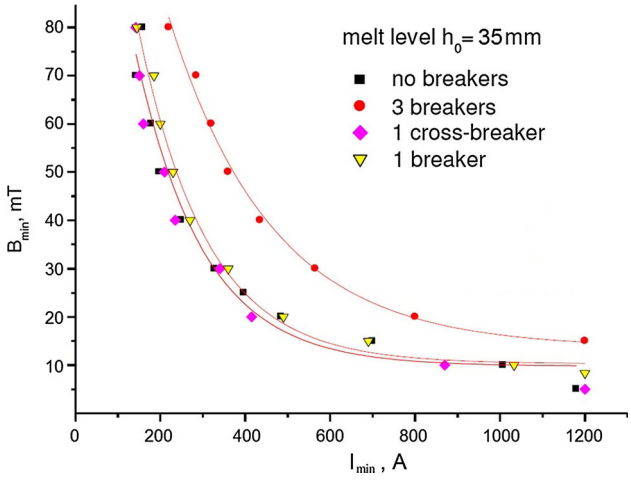

Fig. 7—Stability thresholds for melt level $h_0 = 35$ mm and different WB arrangements.

amplitude of oscillations grows linearly with respect to the anode current; however, its sensitivity to the change in magnetic field B is different: at low B values, the growth is close to linear, but then saturates at higher magnetic field.

Now we take the first melt level, $h_0 = 20$ mm, fix magnetic field at about the midrange $B = 50$ mT, and introduce several WB configurations. Figure 5 shows the obtained surface oscillations with none, one and three WB, arranged in parallel to each other at equal spacings along the width of the cell (as in Figure 1). As seen from the graph, the addition of even one WB lowers the RMS of oscillations by ~35 pct compared to the control case. Three obstacles reduce the RMS by another ~25 pct. The last curve in Figure 5 has been obtained with "cross-breaker," which consisted of two single WBs, perpendicular to each other and crossing at the center of the cell. One can see that such a WB arrangement is damping oscillations most effectively for $h_0 = 20$ mm, *i.e.*, when the relative height of the obstacle is 0.75 h_0. Indeed, because the superposition of two sloshing modes along each horizontal direction comprises the overall "rolling" wave, such WB configuration is affecting the sloshing in each of these directions. Finally, Figure 6 shows the lower thresholds of the instability for melt level $h_0 = 20$ mm. This confirms the gradual improvement of the melt stability from none to one and three WB cases. The "cross-breaker" case, which showed lowest amplitude of the surface oscillations, from the stability point of view, lies somewhat in between 1 and 3 WB arrangements.

Stability results for $h_0 = 35$ mm are shown in Figure 7. Now the relative WB height is 0.43 h_0, and it is clear that the performance of WB starts to deteriorate: everything below 3 WB has basically no effect on the stability thresholds. Further increase of the number of WBs makes no improvements over 3WB case (we also tested 5WB and 7WB parallel arrangements).

Increasing the melt height even further to $h_0 = 50$ mm results in almost no influence of WBs on the stability thresholds. The relative WB height now is only 0.3 h_0. Figure 8 shows the results of previously most effective 3WB case for this melt level.

The frequency of the free surface oscillations was also found to decrease with the introduction of obstacles in the liquid metal. The frequency spectra of the wave was recovered from the video recordings for two heights of the liquid metal $h_0 = 20$ and 35 mm. The base frequency for the control case without WBs agrees well with the natural frequency of the wave f_0, which can be easily calculated from the expression for the propagation speed c of the internal gravity waves at the interface between two liquids in a shallow binary layer: $c = \sqrt{\Delta\rho g/(\rho_0/h_0 + \rho_1/h_1)}$, where ρ_0 and ρ_1 are densities of the liquid metal and top fluid (water), respectively, $\Delta\rho$ is their difference, g is the acceleration due to gravity, and $h_1 = 5$ cm is the height of the top fluid. The base frequency f_0, Hz, of the wave is then obtained as $f_0 = c/\lambda$, where $\lambda = 0.6$ m is the wave length (half of the cell perimeter). Thus, the calculated base frequencies are $f_0 = 0.66$ Hz for $h_0 = 20$ mm and $f_0 = 0.85$ Hz for

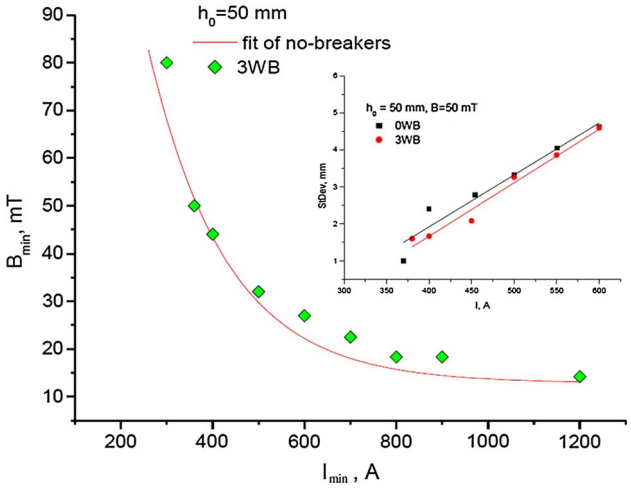

Fig. 8—Stability thresholds for $h_0 = 50$ mm: no-WB (solid line) and 3WB. Insert shows the 3WB influence on the RMS value of surface oscillations vs. no-WB case for $h_0 = 50$ mm.

Table I. Base Frequency f_0 of the Wave Measured for Different WB Configurations at Two Heights h_0 of the Liquid Metal Layer

Configuration	f_0, Hz ($h_0 = 20$ mm)	f_0, Hz ($h_0 = 35$ mm)
No-WB	0.67	0.86
1 WB	0.65	0.84
3 WB	0.58	0.79
1 cross-WB	0.57	0.77

$h_0 = 35$ mm. They are in a very good agreement with the ones observed experimentally, see Table I, which shows experimental values of f_0 for different WB configurations.

The experimental tests investigating the influence of the different configurations of "wave-breakers" on the rolling-pad surface instability were performed in the low-temperature laboratory model. The effectiveness of these configurations was assessed by analyzing the data of the stability thresholds and the RMS values of the free surface oscillations. At the high relative height of the obstacles (0.75 h_0), the pronounced suppression of the waves was observed: up to 50 pct (for 3WB) by RMS value. In this case, the frequency of the wave (hence its celerity) was also found to decrease by ~15 pct for 3WB and cross-WB cases. For the higher melt level $h_0 = 35$ mm, when the relative height of the obstacles becomes 0.43 h_0, the suppression effect was found to be less pronounced, leaving only 3WB configuration as the only one effective: surface oscillations decreased by ~30 pct (RMS) and the wave propagation speed by 8 pct. Finally, at $h_0 = 50$ mm (WB height is 0.3 h_0), the damping effect of the obstacles was practically unnoticeable.

The outcomes of this study had an important industrial impact: the results were used by Rio-Tinto for the development and validation of the full 3D numerical model of electrolysis cell, which allowed them to increase the productivity of its plants while lowering the environmental footprint. This and the subsequent numerical works[9,10] led to a patent.[11]

REFERENCES

1. A. Pedchenko, S. Molokov, J. Priede, A. Lukyanov, and P.J. Thomas: *EPL*, 2009, vol. 88, p. 24001.
2. S. Renaudier, B. Bardet, G. Steiner, A. Pedcenko, J. Rappaz, S. Molokov, and A. Masserey: *TMS Light Metals*, Wiley, New York, 2013, pp. 577–84.
3. J.F. Gerbeau, C.L. Bris, and T. Lelièvre: *Mathematical Methods for the Magnetohydrodynamics of Liquid Metals*, Oxford University Press, New York, 2006.
4. T. Sele: *Metall. Trans. B*, 1977, vol. 8 (4), pp. 613–18.
5. Y. Song, P. Jianping, D. Yuezhong, W. Yaowu, L. Baokuan, and F. Naixiang: *Metall. Res. Technol.*, 2016, vol. 113, p. 7.
6. M. Dupuis and V. Bojarevics:*TMS Light Metals*, 2014, pp. 479–82.
7. M. Dupuis and V. Bojarevics:*TMS Light Metals*, 2015, pp. 821–26.
8. M. Dupuis and M. Pagé: *TMS Light Metals*, 2016, pp. 909–14.
9. G. Steiner: Simulation numérique de phenomènes MHD: Application l'électrolyse de l'aluminium Thesis number 4469, EPFL, 2009.
10. S. Flotron: Simulations numériques de phénomènes MHD-thermiques avec interface libre dans l'électrolyse de l'aluminium Thesis number 5738, EPFL, 2013.
11. S. Renaudier and B. Bardet: Electrolysis tank with slotted floor. patent WO2015017925, 2013.